Proceedings of the 26th International Conference on
Port and Ocean Engineering under Arctic Conditions
June 14-18, 2021, Moscow, Russia

The numerical modelling of dynamic processes in the ice samples using the grid-characteristic method

P.Stognii[1], V.Epifanov[2], V.Golubev[1], K.Beklemysheva[1], V.Miryaha[1]

[1] MIPT (Moscow institute of physics and technology (National research university), Dolgoprudny, Russia)
[2] IAM RAS (Ishlinsky Institute for Problems in Mechanics of the Russian Academy of Sciences, Moscow, Russia)

ABSTRACT

In this work the numerical and experimental study of wave processes, initiated by the shear loading of an ice sample, was carried out. Waves generated during the shock impact on the back surface of ice with a truncated cone-shape indenter were investigated. The wave fields inside the ice at consistent time moments were calculated. For presenting the computed results, the isosurfaces of the velocity vector and all components of the stress tensor were used. The numerical solution of the circular tear-off fracture problem under the influence of loads, affecting at opposite surfaces of the cubic ice sample, was obtained. The wave field for the velocity module and all velocity components were calculated with and without taking into account the destruction process. For the numerical modelling, the grid-characteristic method on the structured computational grids was used. The grid-characteristic method was developed and extended for computing wave processes in different continua (deformable solid media, ice, liquid, gas, plasma).

KEY WORDS: Numerical modelling; Grid-characteristic method; Ice loading.

INTRODUCTION

Today the investigation of the Arctic region is very important as large amounts of hydrocarbons are located in this area (Dmitrieva and Romasheva, 2020). Besides, the Northern Sea Route, located in the Arctic region, is a very important connection between different countries (Liu and Kronbak, 2010). Ice formations, such as icebergs, ice fields, are a barrier on the way of study and development of the Arctic (Stognii and Petrov, 2020). During the seismic prospecting works, ice formations bring in extra reflections into the seismograms, which present the seismic velocity distribution. The way, the seismic waves spread through the ice medium, is not trivial because of the complicated structure of ice, which is not homogeneous. Therefore, such characteristics of ice as strength, sound velocity, density, vary within one layer of ice. This fact should be taken into account in the projection of various buildings on the surface of the ice field (Beklemysheva, et al., 2019), while constructing the ice breakers for passing the Northern Sea Route (Kwok, 2018).

In this work we carry out the numerical study of the wave processes in different ice samples with the use of the grid-characteristic method on structured computational grids (Ivanov and Khokhlov, 2019). In the first numerical study, we model shock impact on the back surface of ice with a truncated cone-shaped indenter for the 2D and 3D case. We obtain the wave fields of the velocity modulus distribution and the stress tensor distribution inside the ice sample. In the second numerical experiment, we study the circular tear-off fracture problem under the influence of loads, affecting at opposite surfaces of the cubic ice sample. The distribution of velocities, stresses and fractures are presented for a wide range of parameters. In addition, we demonstrate the experimental results for the described problems and carry out the comparative analysis between the numerical and experimental results.

NUMERICAL METHOD

We used the system of equations for the linear-elastic medium for describing the dynamic behavior of the seismic waves spread in the medium (Khokhlov, et al., 2019):

$$\rho \frac{\partial \mathbf{v}}{\partial t} = (\nabla \cdot \boldsymbol{\sigma})^T \ , \tag{1}$$

$$\frac{\partial \boldsymbol{\sigma}}{\partial t} = \lambda (\nabla \cdot \mathbf{v}) \mathbf{I} + \mu \left((\nabla \times \mathbf{v}) + (\nabla \times \mathbf{v})^T \right) \ , \tag{2}$$

where v is the medium velocity, t is the time, ρ is the medium density, λ and μ are the Lame parameters, $\boldsymbol{\sigma}$ is the Cauchy stress tensor.
The grid-characteristic method was used for solving the system (1, 2) numerically. Firstly, we present the system (1, 2) as:

$$\frac{\partial \mathbf{q}}{\partial t} + \mathbf{A}_x \frac{\partial \mathbf{q}}{\partial x} + \mathbf{A}_y \frac{\partial \mathbf{q}}{\partial y} = 0 \ , \tag{3}$$

where the vector $\mathbf{q}$ is $\mathbf{q} = \{\sigma_{xx}, \sigma_{xy}, \sigma_{yy}, v_x, v_y\}$. The matrixes $\mathbf{A}_x$ and $\mathbf{A}_y$ are made out of the coefficients of the system (1, 2). After splitting the equation (3) in coordinates, we obtain two 1D systems:

$$\frac{\partial \mathbf{q}}{\partial t} + \mathbf{A}_i \frac{\partial \mathbf{q}}{\partial i} = 0, i \in \{x, y\} \ . \tag{4}$$

Now, we examine the system (4) for the coordinate x, which is hyperbolic, then we can rewrite it as:

$$\frac{\partial \mathbf{q}}{\partial t} + \boldsymbol{\Omega}_x \boldsymbol{\Lambda}_x \boldsymbol{\Omega}_x^{-1} \frac{\partial \mathbf{q}}{\partial x} = 0 \ , \tag{5}$$

where the matrix $\boldsymbol{\Omega}_x$ is made of the eigen vectors of the matrix $\mathbf{A}_x$, the matrix $\boldsymbol{\Lambda}_x$ is made of the eigen values of the matrix $\mathbf{A}_x$, which are equal to $\{-c_p, c_p, -c_s, c_s, 0\}$. Here, c_p and c_s can be found from $c_p = \sqrt{(\lambda + 2\mu)/\rho}, c_s = \sqrt{\mu/\rho}$. After the variable change $\mathbf{p} = \boldsymbol{\Omega}_x^{-1} \mathbf{q}$, the system (5) will transfer to:

$$\frac{\partial \mathbf{p}}{\partial t} + \boldsymbol{\Lambda}_x \frac{\partial \mathbf{p}}{\partial x} = 0 \tag{6}$$

The system (6) consists of five independent equations, each of which was solved by the Rusanov scheme of the third order of accuracy (Khokhlov and Golubev, 2019).

In addition, we solved the system of equations (1) – (2) in the radial symmetry formulation of the problem. The equations were solved the same way as for the Cartesian grids, while the rest terms were taken into account using the additional corrector.

SHOCK IMPACT ON THE ICE SAMPLE

We computed resulting stress and velocity fields inside the ice sample in the conditions of hydrostatic compression. Firstly, we calculated the ice sample in the 2D form without any modifications concerning the radial symmetry. The ice characteristics were the following: c_p = 3940 m/s, c_s = 1850 m/s, ρ = 917 kg/m^3 . We modeled the seismic waves spread from the impulse source, described by the Reiker impulse, located on the left center side of the cone. The wave fields of the velocity modulus distribution inside the ice sample at different consequent time moments are presented in Figure 1. The obtained distribution of the velocity modulus is similar to the same distribution of the experimental results (Epifanov, 2020).

a) t = 0.04 s.

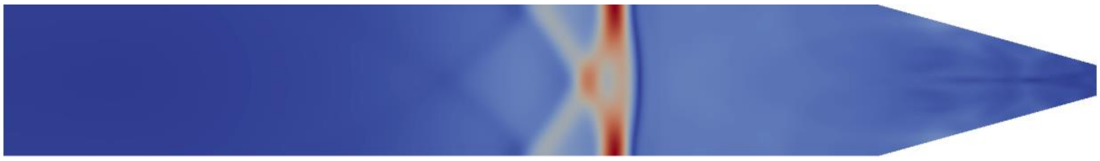

b) t = 0.3 s.

Figure 1. The wave fields of the velocity modulus distribution inside the ice sample at consequent time moments.

Then, we carried out the same computations, taking into account the radial symmetry of the sample. The ice characteristics were the same as in the first model. We computed the seismic waves spread from the impulse source, described by the Reiker impulse, located in the upper center of the cone. The radial symmetry of the cone led to the possibility of the 3D model change by the 2D model. The surrounding medium of ice possessed the following parameters: c_p = 6400 m/s, c_s = 3130 m/s, ρ = 2700 kg/m3 . The computational model is presented in Figure 2, where the ice medium is depicted by the blue color, and the surrounding medium is shown by the red color.
The wave fields of the velocity modulus distribution inside the ice sample at different consequent time moments are presented in Figure 3. The wave fields of the horizontal component of the stress tensor inside the ice sample at consequent time moments are presented in Figure 4.

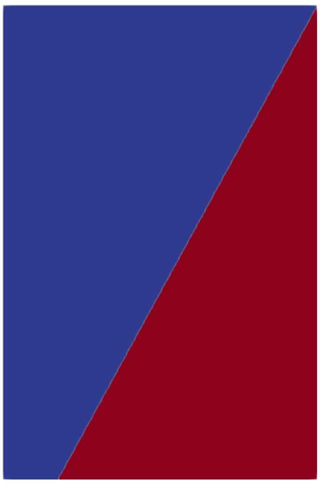

Figure 2. The computational model of the ice cone in the assumption of the radial symmetry of the 3D sample.

a) t = 0 s. b) t = 4.8 * 10^{-6} s. c) t = 9.6 * 10^{-6} s.

Figure 3. The wave fields of the velocity modulus distribution inside the ice sample at consequent time moments.

a) t = 0 s. b) t = 4.8 * 10^{-6} s. c) t = 9.6 * 10^{-6} s.

Figure 4. The wave fields of the horizontal component of the stress tensor inside the ice sample at consequent time moments.

The problem of the dynamic loading of the conical specimen created from ice was successfully simulated. The conoid with the smaller diameter equals to 1 cm, bigger diameter equals to 6 cm and height equals to 20 cm was considered (see Figure 5, left). The ice density was set to 917 kg/m^3, and Lame parameters led to the P-wave and S-wave velocities as c_p = 3940 m/s, c_s = 1850 m/s. The isotropic linear elastic model was used to describe the dynamic behavior of the medium. It was solved numerically on the curvilinear (hexahedral) meshes with the algorithm of the 2nd approximation order (Golubev, et al., 2021). Five different meshes (one per sector and one in a center) covered the region of the interest (see Figure 5, right). The appropriate physically correct contact conditions were set explicitly (Golubev, et al., 2020). On all external surfaces the free boundary condition was applied.

The used grid-characteristic method relies on the explicit solution of linear transport equations for Riemann invariants. It allows us to use only 328 000 nodes for resolving all volumetric and surface waves. The source was simulated by the external force applied at the largest side along *Z*-axis with the Ricker wavelet time dependency. The disturbance time was 200 microseconds, and the total physical time was 300 microseconds. The computational time was 30 minutes on 12 cores of modern CPU processors. To analyze the simulation results the modulus of velocity was saved at each mesh nodes. It was presented at the Figure 6 at successive times: the disturbance initiation, scattering from side surface, scattering from the cone end, back propagation of scattered waves. The presented numerical approach can be used to analyze the wave dynamic of the ice under complex loading conditions.

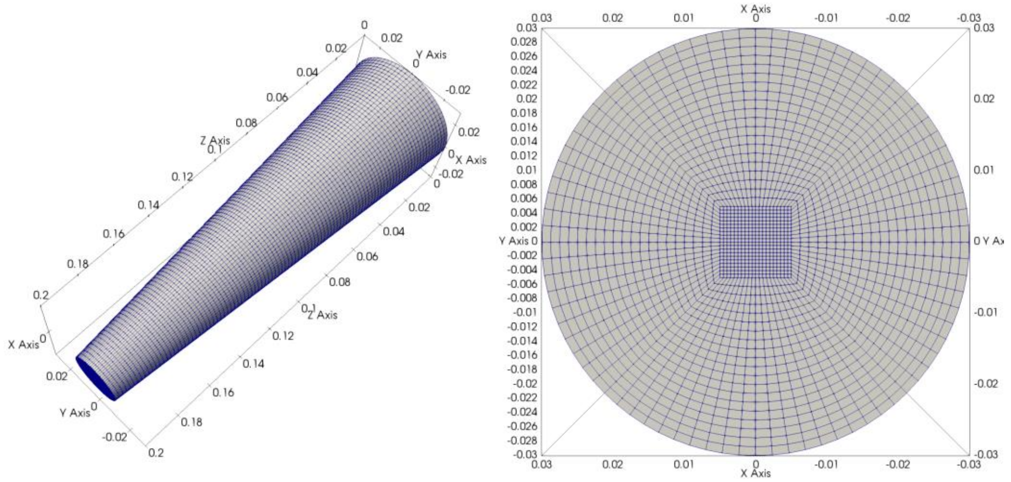

Figure 5. The conoid covered with meshes is depicted. Side view (left) and top view (right).

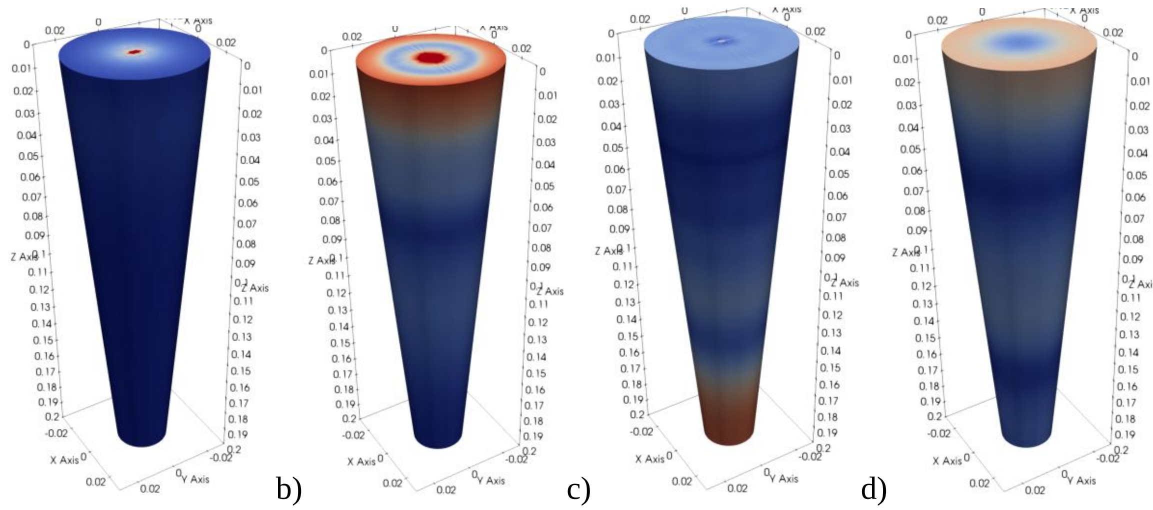

Figure 6. The velocity modulus at successive times: a) the disturbance initiation, b) scattering from side surface, c) scattering from the cone end, d) back propagation of scattered waves.

CIRCULAR TEAR-OFF FRACTURE

For the numerical calculations of tear-off fractures, we used the grid-characteristic method on three-dimensional regular grids.

We used a destructible viscoelastic model of the material, which allows to obtain a fracture pattern that qualitatively coincides with the experiment under shock loading and brittle fracture (Beklemysheva, et al., 2019, Beklemysheva, et al., 2021). A destroyed node is marked, and later in calculation it undergoes a correction after each time step based on Prandtl-Reuss model with a zero plasicity limit. It gives a feedback from the destructed area -- cracked material does not conduct waves in the same way as an intact material. In this model, a layer of failed nodes shields the underlying material from tension and shear elastic waves, only compression waves pass through. The direction of cracks if not considered in this model.

Within the framework of the used implementation of the method, various failure criteria were available to us, including anisotropic ones. To calculate the given formulation, the Tsai-Wu failure criterion was applied, which for an isotropic material is reduced to a combination of the Mises criterion and the maximum tensile stress criterion that cover the basic destruction mechanisms for a brittle medium.

Figure 7 shows experimental data on shock unloading of a cubic ice sample. We attempted different problem statements (Figure 8) to better illustrate dynamic processes inside an ice sample during loading and unloading.

Figure 7. Experimental data on shock unloading of an ice sample.

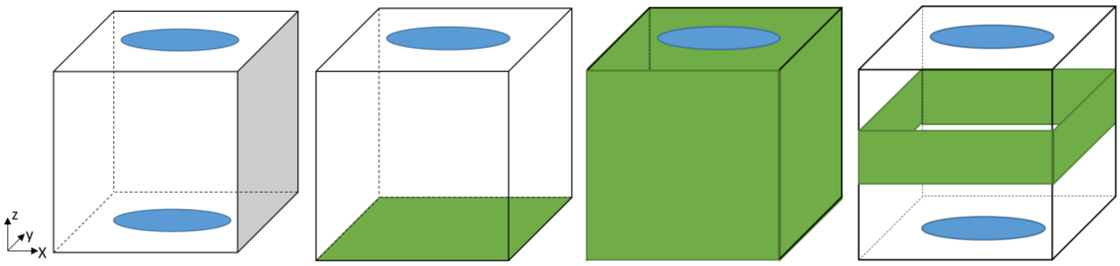

Figure 8. General view of problem statements: a - two indenters; b – one indenter and the fixed lower boundary; c – one indenter and fixed boundaries; d – two indenters and an area with fixed boundary.

A cubic ice sample was considered, and a force was applied to the circular areas on the upper and lower faces, which for a relatively long time (relative to the times of acoustic processes) increased to a certain maximum value. After that, it instantly dropped to zero. The following material parameters were used: Lame parameters $\lambda = 2.9$ MPa and $\mu = 5.7$ MPa, density $\rho = 0.917$ g / cm3. Various values of ice strength thresholds, maximum load and time during which this maximum load was reached were considered.

The pictures of the distribution of velocities, stresses and fractures were obtained during the calculation for a wide range of different parameters. The most characteristic shape, which was obtained in a series of numerical experiments, turned out to be a disk crack. During the first passage of elastic waves from the areas of application of the external force through the center and their interference, a small flat horizontal disc-shaped crack is formed. In the second pass, a characteristic flat horizontal ring-shaped crack is formed, slightly separated from the central disk-shaped crack. By varying the strength values of the material, multiple axial cracks can also be produced. For solving the problem of obtaining the tear-off fracture, the experiment on shock unloading on the ice sample was carried out (Epifanov, 2007). For this, the indenter of the cylindrical form was pressed in the upper side of the ice cube. The experimental results are shown in Figure 12, where the tear-off fracture is located in the center of the ice cube.

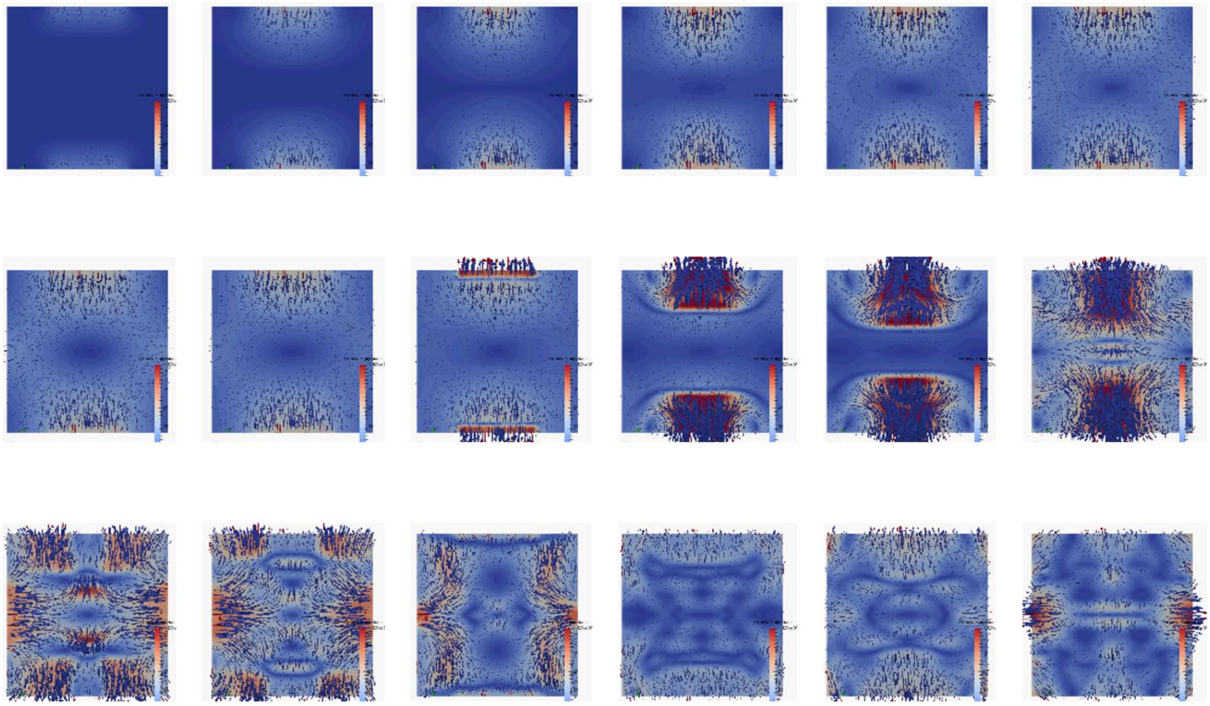

Figure 9. Typical wave pattern (vector and modulus of velocity at each node) when calculating the shock unloading of a cubic sample. Under slow loading, waves practically do not arise in the medium, and the velocities are rather low. During the subsequent shock unloading (middle of the second row), elastic waves of large amplitude appear, which interfere in the investigated volume.

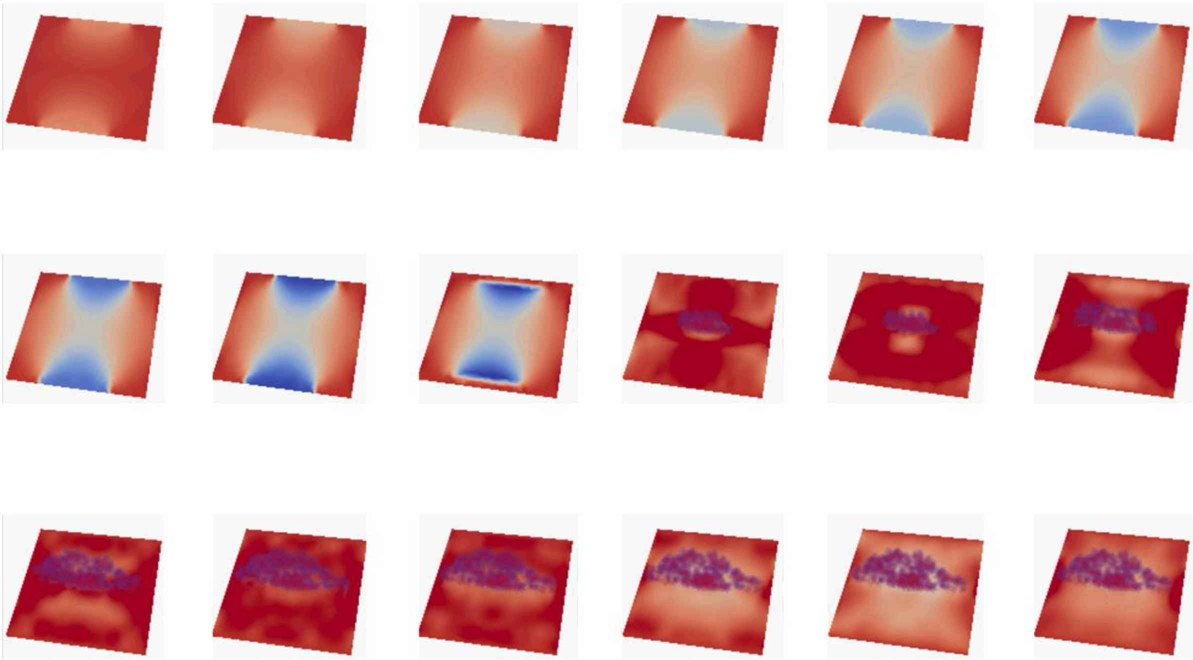

Figure 10. Disc crack. The most typical shape, which was obtained in a series of numerical experiments. During the first passage of elastic waves from the areas of application of the external force through the center and their interference, a small flat horizontal disc-shaped crack is formed. In the second pass, a typical flat horizontal ring-shaped crack is formed, slightly separated from the central disk-shaped crack.

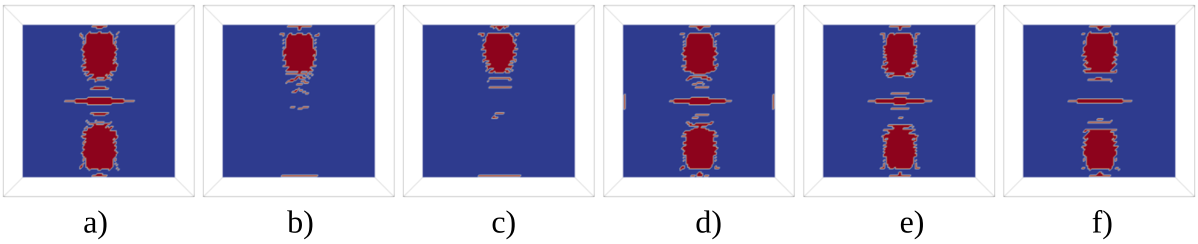

Figure 11. The influence of border conditions. Failed nodes on an XZ plane: a - two indenters; b – one indenter and the fixed lower boundary; c – one indenter and fixed boundaries; d – two indenters and an area with a fixed boundary 10% height; e – two indenters and an area with a fixed boundary 20% height; f – two indenters and an area with a fixed boundary 30% height.

Figure 12. Experimental results. The ice sample with the tear-off fracture in the center.

Within the framework of the considered model and formulation, it was not possible to achieve an exact correspondence with the experiment. An annular crack was reproduced (Figures 9-11), but, in contrast to the experiment (Figures 7, 12), in its center there was always a fracture region, which appeared earlier, during the first passage of elastic waves. Within the framework of changing the calculation parameters within the framework of the model, it is impossible to eliminate the disk crack while retaining the annular crack. Hashin and Tsai-Hill failure criteria were also considered, but did not show any significantly different patterns. We plan to work on Drucker-Prager and Puck criteria, but they require additional material parameters that cannot be measured directly in an experiment.

CONCLUSIONS

In this work we presented the results of numerical modelling of wave processes in the ice samples with the use of the grid-characteristic method. The wave fields of the velocity and stress tensor for the problem of modelling the shock impact on the back surface of ice with the truncated cone shape were obtained for the 2D and 3D case. Then, we carried out the numerical study of the circular tear-off fracture problem under the influence of loads on the ice sample of the cubic form. The comparative analysis between the numerical and experimental results for the described problems proved the correct application of the grid-characteristic method to the study of the ice samples under different loads, though the complete coincidence was not obtained. The work needs to be continued in order to reveal the better coincidence between the numerical and experimental results.

ACKNOWLEDGEMENTS
The reported study was funded by the Russian Foundation for Basic Research, project no. 20-01-00649.

REFERENCES

Beklemysheva, K., Golubev, V., Petrov, I., Vasyukov, A., 2021. Determining effects of impact loading on residual strength of fiber-metal laminates with grid-characteristic numerical method. *Chinese Journal of Aeronautics*, 34(7), pp. 1-12.

Beklemysheva, K., Ermakov, A., Favorskaya, A., 2019. Numerical simulation of cone object destruction under a short high-energy pulse. *Procedia Computer Science*, 159, pp.1095-1102.

Dmitrieva, D., Romasheva, N., 2020. Sustainable Development of Oil and Gas Potential of the Arctic and Its Shelf Zone: The Role of Innovations. *J. Mar. Sci. Eng., 8*, 1003.

Epifanov, V.P., 2007. Physical mechanisms of ice contact fracture. *Dokl. Phys.,* 52, pp.19–23.

Epifanov, V.P., 2020. Contact fracture behavior of ice. *Ice and Snow*, 60(2), pp.274-284.

Golubev, V., Shevchenko, A., Petrov, I., 2020. Simulation of Seismic Wave Propagation in a Multicomponent Oil Deposit Model. *International Journal of Applied Mechanics*, 12(8), № 2050084.

Ivanov, A.M., Khokhlov, N.I., 2019. Efficient Inter-process Communication in Parallel Implementation of Grid-Characteristic Method. In: Petrov I., Favorskaya A., Favorskaya M., Simakov S., Jain L. eds., Smart Modeling for Engineering Systems. *GCM50 2018*. Smart Innovation, Systems and Technologies, 133, https://doi.org/10.1007/978-3-030-06228-6_9

Khokhlov, N.I., Golubev, V.I., 2019. On the Class of Compact Grid-Characteristic Schemes. In: Petrov I., Favorskaya A., Favorskaya M., Simakov S., Jain L. eds., Smart Modeling for Engineering Systems. *GCM50 2018*. Smart Innovation, Systems and Technologies, 133. 10.1007/978-3-030-06228-6_7

Khokhlov, N.I., Stetsyuk, V.O., Mitskovets, I.A., 2019. Overset grids approach for topography modeling in elastic-wave modeling using the grid-characteristic method. *Computer Research and Modeling*, 11(6), pp.1049–1059.

Kwok, R., 2018. Arctic sea ice thickness, volume, and multiyear ice coverage: Losses and coupled variability (1958-2018). *Environmental Research Letters*, 13(10).

Liu, M., Kronbak, J., 2010. The potential economic viability of using the Northern Sea Route (NSR) as an alternative route between Asia and Europe. *Journal of Transport Geography*, 18(3), pp.434-444.

Stognii, P.V., Petrov, I.B., 2020. Numerical modelling of seismic waves spread in models with an ice field in the arctic shelf. *Computer Research and Modeling*, 12(1), pp.73-82.